VIP Hydrogen Bonds

DOI: 10.1002/anie.201203296

Watching Water Migration around a Peptide Bond**

Kohei Tanabe, Mitsuhiko Miyazaki, Matthias Schmies, Alexander Patzer, Markus Schütz, Hiroshi Sekiya, Makoto Sakai, Otto Dopfer, and Masaaki Fujii**

Life is believed to have its origin in aqueous environments, and 70% of our body consists of water. The essential components of biological systems have to interact in aqueous solutions with water molecules by intermolecular forces, such as hydrogen bonds, dispersion forces, and hydrophilic/hydrophobic interactions.[1] Proteins are one of the most important biological supramolecules and offer at the CO and NH sites of the -CONH- linkages of the peptide chain attractive hydrogen-bonding sites, in which H_2O can act either as a proton donor or a proton acceptor, respectively. The solvation of a protein has a strong effect on its molecular shape, and as a consequence the fluctuations of the water network on the surface have important influence on its folding properties and catalytic function.[2] Most fundamentally, when a protein starts its folding motion, the water network hydrogen-bonded to the protein has to rearrange and thus affects the dynamics. Therefore, up-to-date quantum chemical simulations on protein folding and its functions include water molecules explicitly.[2h,l,m] A deeper understanding of these phenomena at the molecular level requires the characterization of the dynamical processes of individual water molecules interacting with the protein. However, most experiments yield only indirect dynamical information averaged over water molecules in the first hydration layer and thus only a tentative and often controversial interpretation of the underlying mechanisms.[2a,e–g,i,k,n] Measurements visualizing the motion of a specific water molecule in a real biological environment are challenging, and so far no experimental data have been reported yet. Such dynamical experiments need to distinguish between each single water molecule, which can bind to numerous different binding sites of the protein and readily exchange their role with other H_2O molecules in the same or higher hydration solvation layers. This inherent complexity of the hydrated protein has so far prevented measurements of the migration of individual water molecules in solution, and therefore nearly all information about such processes relies on theoretical approaches.[2a,f–h,l-o]

Although quantum chemical simulations for such complex systems have substantially progressed in recent years because of rapid computer developments, their accuracy is still rather limited and experimental benchmark data for model systems are highly requested for calibration purposes. To this end, we have developed in the past decade an experimental strategy for the investigation of dynamical intermolecular processes,[3] which typically occur on the picosecond (ps) time scale. This approach involves the generation of molecular clusters isolated in supersonic beams and the characterization of their dynamics using ps time-resolved IR spectroscopy. The fruitful combination of spectroscopy and quantum chemistry currently provides the most direct and most detailed access to intermolecular interactions.[1] IR spectroscopy is particularly sensitive to structural motifs.[4] In initial benchmark experiments, we developed a three-color UV-UV-IR tunable picosecond pump–probe laser spectrometer[3a,b,e,g] and measured the ionization-induced $\pi \rightarrow$H site switching dynamics of rare gas ligands attached to phenol.[3a–d,5] In this case, the position of the ligand was monitored by the structure-sensitive frequency of the phenolic OH stretching vibration. Although for a very limited number of water complexes with aromatic molecules the laser-induced migration of the water ligand has recently been inferred from "static" spectroscopy using nanosecond lasers,[4b,d,6] no time-resolved studies about the dynamics of this fundamental process have been reported yet.[3a]

We have applied our ps pump–probe approach to the *trans*-acetanilide–H_2O (AA-H_2O) cluster to monitor the water migration dynamics around a peptide linkage by the time evolution of the IR spectra measured at a delay time Δt after the ionization event (Figure 1). AA is one of the smallest aromatic molecules with a -CONH- peptide bond (Figure 1) and thus serves as a suitable model for proteins and related biomolecules. It can form two different types of hydrogen bonds with water, resulting in NH- and CO-bound isomers, which can readily be distinguished by their different IR and electronic spectra[6a,7] (see the Supporting Information). The "static" IR spectrum of the CO-bound isomer (reactand R) in the neutral ground state (S_0) measured by nanosecond lasers ($\Delta t = -50$ ns, Figure 2) reveals a sharp band at 3473 cm^{-1} and a broader one at 3496 cm^{-1} assigned to the free NH stretching vibration (ν_{NH}^{f}) and the hydrogen-bonded OH stretching mode (ν_{OH}^{b}) of the water ligand, respectively.[6a] The corresponding picosecond IR spectra before photoionization

[*] K. Tanabe, Dr. M. Miyazaki, Prof. Dr. M. Sakai, Prof. Dr. M. Fujii
Chemical Resources Laboratory, Tokyo Institute of Technology
Yokohama 226-8503 (Japan)
E-mail: mfujii@res.titech.ac.jp
M. Schmies, A. Patzer, M. Schütz, Prof. Dr. O. Dopfer
Institut für Optik und Atomare Physik
Technische Universität Berlin, 10623 Berlin (Germany)
E-mail: dopfer@physik.tu-berlin.de
Prof. Dr. H. Sekiya
Graduate School of Science, Kyushu University
Fukuoka 812-8581 (Japan)

[**] This study was supported by the MEXT (priority area 477 Japan), the Core-to-Core Program of the JSPS, and the DFG (grant number DO 729/4). We thank Kenji Sakota (Kyushu University) and Shun-ichi Ishiuchi (Tokyo Institute of Technology) for stimulating discussions. M. Schmies is grateful for an Elsa Neumann fellowship.

Supporting information for this article is available on the WWW under http://dx.doi.org/10.1002/anie.201203296.

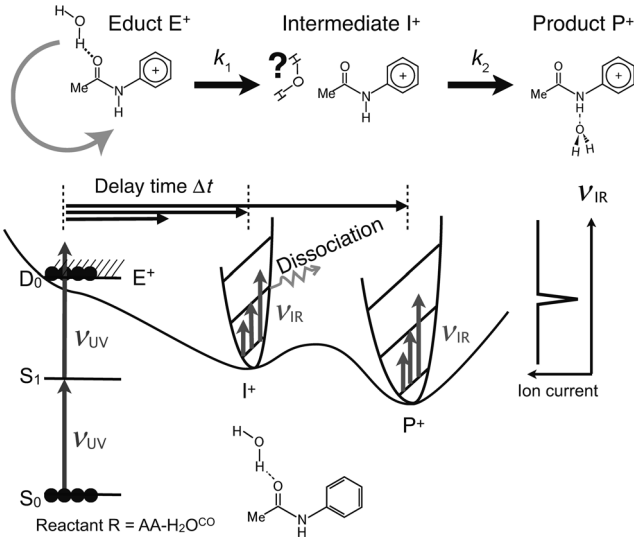

Figure 1. Strategy of picosecond time-resolved IR dip spectroscopy, along with reaction model M1.

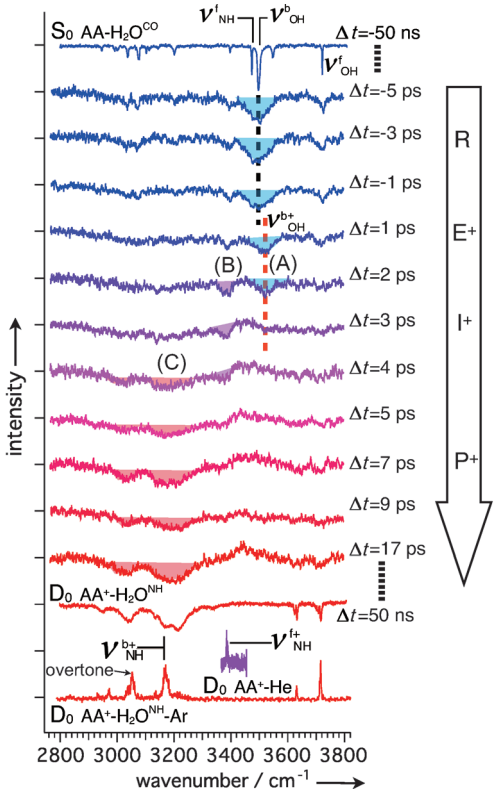

Figure 2. Time-resolved IR dip spectra of AA^+-H_2O. The spectra at $\Delta t = -50$ and 50 ns are "static" IR spectra of the CO-bound and NH-bound isomers in the neutral and cationic states measured by nanosecond lasers. The IR spectra of cold AA^+-He and AA^+-H_2O-Ar clusters generated by electron impact ionization are also shown for comparison. See the text and the Supporting Information for details.

($\Delta t<0$) are the same, except for the lower spectral resolution (about 15 cm^{-1}) arising from the shorter laser pulse duration (about 3 ps).

As the NH- and CO-bound isomers of AA-H_2O have different S_1 energies,[6a,7] the latter one can selectively be ionized by resonant two-photon UV-UV ionization ($\Delta t = 0$, Figure 1, Figure S4 in the Supporting Information). The ps IR spectra change immediately after ionization ($\Delta t = 1$ and 2 ps, Figure 2). The ν_{OH}^{b+} band of the initial structure after ionization (educt E^+) is shifted from ν_{OH}^{b} by 28 cm^{-1} to a higher frequency, which means that hydrogen bonding to the CO site is weakened by ionization, mainly because of charge–dipole repulsion.[6f,8] The ν_{OH}^{b+} transition becomes weaker at $\Delta t = 2$ ps and disappears after $\Delta t = 3$ ps. After $\Delta t =$ 4 ps, a new broad band appears near 3200 cm^{-1} and grows with increasing delay. Finally, the spectrum at $\Delta t = 17$ ps has converged and resembles the "static" one observed at $\Delta t =$ 50 ns after ionization recorded by nanosecond lasers. The broad 3200 cm^{-1} band was assigned to the bound NH stretching vibration (ν_{NH}^{b+}) arising from hydrogen bonding to H_2O,[6a] and is the spectral signature of the final reaction product P^+ (Figure 1). Therefore, the disappearance of ν_{OH}^{b+} and the subsequent appearance of ν_{NH}^{b+} unambiguously demonstrate the direct observation of the water migration from the CO to the NH site of the peptide bond in AA^+.

Significantly, the IR spectrum at $\Delta t = 3$ ps shows a unique trend and spectral features not observed in the other spectra. The ν_{OH}^{b+} band of the CO-bound H_2O ligand disappears but the ν_{NH}^{b+} band of the NH-bound ligand has not yet appeared. Instead, this spectrum shows a new band at 3385 cm^{-1} assigned to the free NH stretching mode of AA^+ (ν_{NH}^{f+}), as inferred from the experimental AA^+-He spectrum (Figure 2). This observation that H_2O has already been released from the CO site at $\Delta t = 3$ ps but has not yet arrived at the NH site provides clear-cut evidence for the existence of an intermediate I^+, which has a structure different from the initial educt E^+ and the final product P^+. Thus, the water migration reaction in AA^+-H_2O involves at least a two-step three-state mechanism, as illustrated in Figure 1.

To shed further light on the details of the water migration dynamics, time evolution curves were measured at three relevant vibrational frequencies (Figure 3). The time evolution at 3495 cm^{-1} (A) represents the overlapping decay of R (reactant) and E^+. The 3385 cm^{-1} transition (B) reflects mainly ν_{NH}^{f+} of I^+ and E^+, whereas the 3185 cm^{-1} band (C) arises from ν_{NH}^{b+} of P^+.

The observed time evolution curves were simulated by the most simple two-step three-state reaction model (model M1, Figure 1) using the following rate equations [Eqs. (1)–(3)]:

$$\frac{d[E^+]}{dt} = -k_1[E^+] \quad (1)$$

$$\frac{d[I^+]}{dt} = k_1[E^+] - k_2[I^+] \quad (2)$$

$$\frac{d[P^+]}{dt} = k_2[I^+] \quad (3)$$

Here, [X] are the populations of X, and k_1 and k_2 are rate constants ($k_i = 1/\tau_i$) for the first and the second step of the reaction (Figure 1). $u(t)$ is the unit step function, and the time profile of the lasers determined by cross-correlation measure-

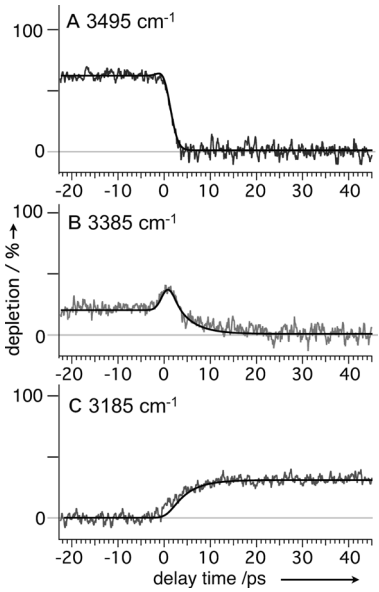

Figure 3. Experimental time evolution curves of three vibrational frequencies of AA^+-H_2O and corresponding fits (model M1, Figure 1).

ments corresponds to 2.8 ps (see the Supporting Information). The rate Equations (1)–(3) are solved by Equations (4)–(7):

$$[R] = 1 - u(t) \tag{4}$$

$$[E^+] = \exp(-k_1 t)u(t) \tag{5}$$

$$[I^+] = \frac{k_1}{k_1 - k_2}[\exp(-k_2 t) - \exp(-k_1 t)]u(t) \tag{6}$$

$$[P^+] = \frac{1}{k_1 - k_2}\{k_1[1 - \exp(-k_2 t)] - k_2[1 - \exp(-k_1 t)]\}u(t) \tag{7}$$

Fits to the experimental time profiles in Figure 3 yield $\tau_1 = (0.7 \pm 0.1)$ and $\tau_2 = (3.7 \pm 0.3)$ ps, and their good agreement with the experimental ones strongly support the existence of the intermediate I^+. Interestingly, τ_1 is of the order of the rotational periods of isolated H_2O estimated from its rotational constants (about 0.4–1.2 ps).

The ps IR spectra in Figure 2 show that all ionized CO-bound clusters (R, E^+) are converted to NH-bound clusters (P^+) with 100% yield. As the clusters are isolated systems without the possibility of energy release, the $P^+ \rightarrow E^+$ back reaction may be expected and has indeed been observed for phenol$^+$-Kr.[5] In this cluster, the Kr atom switches the initial binding site from the aromatic π ring to hydrogen-bonded OH site by ionization, however the $H \rightarrow \pi$ back reaction eventually leads to a nonvanishing [π]/[H] equilibrium population ratio. For AA^+-H_2O, the lack of any back reaction and unity yield for the $E^+ \rightarrow P^+$ forward reaction indicates that efficient intracluster vibrational energy redistribution (IVR) in P^+ prevents the $P^+ \rightarrow E^+$ back reaction because of fast removal of vibrational energy from the reaction coordinate. The time evolution of the width of the $\nu_{NH}{}^{b+}$ band is also consistent with IVR in P^+.[3c] Unfortunately, the internal energies in AA^+-H_2O before and after water migration are unknown, as structured photoionization spectra could not be obtained for the CO-bound isomer.[7] However, they must be high enough so that the low-frequency inter- and intramolecular vibrations can act as efficient bath modes for IVR. A more detailed rate equation analysis including IVR (model M2) further improves the functions fitted to the experimental time evolution curves, but essentially provides the same overall water migration time of about 5 ps. Comparison of the IR spectrum of AA^+-H_2O generated by photoionization and subsequent $E^+ \rightarrow P^+$ isomerization ($\Delta t = 50$ ns) with the corresponding IR spectrum of cold AA^+-H_2O-Ar (Ar-tagged P^+) in Figure 2 clearly indicates the substantial internal energy content of the reaction product P^+ (Figure S3 in the Supporting Information).

In summary, the dynamics of water migration around a peptide bond was measured as about 5 ps using time-resolved IR spectroscopy of AA^+-H_2O. Significantly, the existence of an intermediate I^+ was revealed, an observation which completely escaped previous "static" IR spectra.[6a] As I^+ does not exhibit any hydrogen bonding to the CO and NH sites, the water ligand must be located outside the -CONH- plane, and possible candidates include binding sites at the phenyl ring and the methyl group. Density functional calculations[9] detailed in the Supporting Information predict the NH-bound structure (P^+) as the most stable minimum (Figure 1), whereas the aromatic CH and aliphatic CH_3 sites are significantly less stable local minima. No minimum was found at the CO site and above the phenyl and amide groups of AA^+. According to these calculations, I^+ corresponds to the CH and/or CH_3 binding site, and thus the H_2O ligand migrates in the molecular plane from the CO to the NH site. Further detailed analysis requires more sophisticated theoretical calculations including molecular dynamics (MD) simulations on a highly accurate multidimensional potential energy surface (with the ionization excess energy as parameter) and wave packet dynamics for inclusion of quantum effects.[3a,6f,10] Currently, no dynamical calculations have been reported for AA^+-H_2O. MD simulations for the related formanilide-H_2O cation, derived from AA^+-H_2O by $CH_3 \rightarrow H$ substitution, actually predict H_2O migration from the CO to the NH site upon ionization.[6f,8] However, in stark contrast to the present experimental evidence, 1) the calculated time constant is on the sub-picosecond time scale, 2) the $P^+ \rightarrow E^+$ back reaction is predicted, and 3) no evidence for an intermediate structure I^+ was presented.[8] These severe deficiencies urgently call for the development and application of more sophisticated theoretical approaches and emphasize the importance of the current experimental results. Experimentally, the next step includes the characterization of microhydrated AA-$(H_2O)_n$ clusters to probe the dynamics of a larger hydration network around proteins at the molecular level,[6b] as well as an extension to polypeptides.

Experimental Section

The principle and setup for the measurement of the ps time-resolved UV-UV-IR ion dip (TRIR) spectra (see Figure S1 in the Supporting Information) are described in detail elsewhere.[3a] Briefly, AA-H_2O clusters are produced in a supersonic jet by expanding AA vapor at

$T = 363$ K seeded in He gas (3.5 bar) with water vapor (2.9 mbar) through a pulsed valve into a vacuum chamber. Neutral AA-H_2O dimers are ionized from the neutral ground state (S_0) employing resonant one-color two-photon ionization (R2PI) through the first excited singlet state (S_1) using a ps UV laser, ν_{UV} (Figure 1). The ions generated in the cation ground state (D_0) are extracted into a time-of-flight mass spectrometer. While monitoring the mass-selected AA^+-H_2O signal, a tunable ps IR laser, ν_{IR}, is fired and scanned through the vibrational range (2800–3800 cm^{-1}) with an adjustable delay (Δt) with respect to the ionizing UV laser, ν_{UV}. The ion signal is amplified, integrated, and monitored as a function of ν_{IR} and/or Δt. When ν_{IR} is resonant with a vibrational transition of AA^+-H_2O, the cluster dissociates upon vibrational excitation, causing a depletion (dip) in the ion current. Thus, the IR spectrum of AA^+-H_2O is obtained by monitoring the depletion of the ion current as a function of ν_{IR}. The generation of the ps UV and IR laser pulses is described elsewhere.[3a] The key parameters are 10 Hz repetition rate, about 3 ps pulse widths, about 15 cm^{-1} spectral widths, and pulse energies of 5 and 70 μJ for ν_{UV} and ν_{IR}, respectively. The UV and the IR laser beams are combined coaxially and focused by a CaF_2 lens with 300 mm focal length into the supersonic molecular beam. Similar R2PI and IR depletion experiments have also been performed using standard IR/UV nanosecond lasers, as described in detail previously.[3a]

Received: April 29, 2012
Published online: June 15, 2012

Keywords: hydrogen bonds · hydration · IR spectroscopy · isomerization · peptides

[1] a) P. Hobza, K. Müller-Dethlefs, *Non-covalent interactions*, The Royal Society of Chemistry, Cambridge, **2010**; b) K. Müller-Dethlefs, P. Hobza, *Chem. Rev.* **2000**, *100*, 143 – 168; c) J. P. Schermann, *Spectroscopy and modelling of biomolecular building blocks*, Elsevier, Amsterdam, **2008**.

[2] a) B. Bagchi, *Chem. Rev.* **2005**, *105*, 3197 – 3214; b) P. Ball, *Chem. Rev.* **2008**, *108*, 74 – 108; c) P. Ball, *Nature* **2011**, *478*, 467 – 468; d) M. Chaplin, *Nature* **2006**, *7*, 861 – 866; e) V. P. Denisov, B.-H. Jonsson, B. Halle, *Nat. Struct. Mol. Biol.* **1999**, *6*, 253 – 260; f) M. Grossman, B. Born, M. Heyden, D. Tworowski, G. B. Fields, I. Sagi, M. Havenith, *Nat. Struct. Mol. Biol.* **2011**, *18*, 1102 – 1108; g) B. Halle, *Philos. Trans. R. Soc. London Ser. B* **2004**, *359*, 1207 – 1224; h) A. Mitsutake, Y. Sugita, Y. Okamoto, Biopolymers **2001**, *60*, 96 – 123; i) N. V. Nucci, M. S. Pometun, A. J. Wand, *Nat. Struct. Mol. Biol.* **2011**, *18*, 245 – 249; j) G. Otting, E. Liepinsh, K. Wüthrich, *Science* **1991**, *254*, 974 – 980; k) S. K. Pal, A. H. Zewail, *Chem. Rev.* **2004**, *104*, 2099 – 2123; l) D. E. Shaw, P. Maragakis, K. Lindorff-Larsen, S. Piana, R. O. Dror, M. P. Eastwood, J. A. Bank, J. M. Jumper, J. K. Salmon, Y. Shan, W. Wriggers, *Science* **2010**, *330*, 341 – 346; m) T. Yoda, Y. Sugita, Y. Okamoto, *Biophys. J.* **2010**, *99*, 1637 – 1644; n) D. Zhong, *Adv. Chem. Phys.* **2009**, *143*, 83 – 149; o) D. Chandler, *Nature* **2005**, *437*, 640 – 647.

[3] a) M. Fujii, O. Dopfer, *Int. Rev. Phys. Chem.* **2012**, *31*, 131 – 173; b) S. Ishiuchi, M. Sakai, Y. Tsuchida, A. Takeda, Y. Kawashima, M. Fujii, O. Dopfer, K. Müller-Dethlefs, *Angew. Chem.* **2005**, *117*, 6305 – 6307; *Angew. Chem. Int. Ed.* **2005**, *44*, 6149 – 6151; c) S. Ishiuchi, M. Sakai, Y. Tsuchida, A. Takeda, Y. Kawashima, O. Dopfer, K. Müller-Dethlefs, M. Fujii, *J. Chem. Phys.* **2007**, *127*, 114307 – 114317; d) S. Ishiuchi, M. Miyazaki, M. Sakai, M. Fujii, M. Schmies, O. Dopfer, *Phys. Chem. Chem. Phys.* **2011**, *13*, 2409 – 2416; e) S. Ishiuchi, M. Sakai, K. Daigoku, T. Ueda, T. Yamanaka, K. Hashimoto, M. Fujii, *Chem. Phys. Lett.* **2001**, *347*, 87 – 92; f) M. Sakai, S. Ishiuchi, M. Fujii, *Eur. Phys. J. D* **2002**, *20*, 399 – 402; g) S. Ishiuchi, M. Sakai, K. Daigoku, K. Hashimoto, M. Fujii, *J. Chem. Phys.* **2007**, *127*, 234304 – 234311.

[4] a) E. Garand, M. Z. Kamrath, P. A. Jordan, A. B. Wolk, C. M. Leavitt, A. B. McCoy, S. J. Miller, M. A. Johnson, *Science* **2012**, *335*, 694 – 698; b) J. R. Clarkson, E. Baquero, V. A. Shubert, E. M. Myshakin, K. D. Jordan, T. S. Zwier, *Science* **2005**, *307*, 1443 – 1446; c) A. Gutberlet, G. Schwaab, O. Birer, M. Masia, A. Kaczmarek, H. Forbert, M. Havenith, D. Marx, *Science* **2009**, *324*, 1545 – 1548; d) M. Miyazaki, A. Fujii, T. Ebata, N. Mikami, *Science* **2004**, *304*, 1134 – 1137; e) J. W. Shin, N. I. Hammer, E. G. Diken, M. A. Johnson, R. S. Walters, T. D. Jaeger, M. A. Duncan, R. A. Christie, K. D. Jordan, *Science* **2004**, *304*, 1137 – 1140.

[5] M. Miyazaki, A. Takeda, S. Ishiuchi, M. Sakai, O. Dopfer, M. Fujii, *Phys. Chem. Chem. Phys.* **2011**, *13*, 2744 – 2747.

[6] a) K. Sakota, S. Harada, Y. Shimazaki, H. Sekiya, *J. Phys. Chem. A* **2011**, *115*, 626 – 630; b) K. Sakota, Y. Shimazaki, H. Sekiya, *Phys. Chem. Chem. Phys.* **2011**, *13*, 6411 – 6415; c) H. M. Kim, K. Y. Han, J. Park, G. S. Kim, S. K. Kim, *J. Chem. Phys.* **2008**, *128*, 041104 – 041106; d) O. Dopfer, *Z. Phys. Chem.* **2005**, *219*, 125 – 168; e) M. Gerhards, A. Jansen, C. Unterberg, A. Gerlach, *J. Chem. Phys.* **2005**, *123*, 074320 – 074330; f) T. Ikeda, K. Sakota, Y. Kawashima, S. Yuiga, H. Sekiya, *J. Phys. Chem. A* **2012**, DOI: 10.1021/jp301804w.

[7] S. Ullrich, K. Müller-Dethlefs, *J. Phys. Chem. A* **2002**, *106*, 9188 – 9195.

[8] H. Tachikawa, M. Igarashi, T. Ishibashi, *J. Phys. Chem. A* **2003**, *107*, 7505 – 7513.

[9] M. J. Frisch, et al., Gaussian 09 Revision A. 02 (Gaussian, Wallingford CT, **2009**). See the Supporting Information.

[10] a) C. Walter, R. Kritzer, A. Schubert, C. Meier, O. Dopfer, V. Engel, *J. Phys. Chem. A* **2010**, *114*, 9743 – 9748; b) S. D. Ivanov, O. Asvany, A. Witt, E. Hugo, G. Mathias, B. Redlich, D. Marx, S. Schlemmer, *Nat. Chem.* **2010**, *2*, 298 – 302.

